Numerical Modelling of a Planing Craft With a V-shaped spray interceptor Arrangement in Calm Water

Mikloš LAKATOŠ [a,1], Kristjan TABRI [a,] Abbas DASHTIMANESH [a] and Henrik ANDREASSON [b]
[a] *Tallinn University of Technology, Estonia*
[b] *Flow Naval Architects AB, Sweden*

Abstract. V-shaped spray interceptors are a novel concept of spray deflection on planing craft. Conventional spray rails are positioned longitudinally on the bottom of the hull and detach the spray from hull deflecting it towards the sides or slightly down and aftward. The V-shaped spray interceptors, on the other hand, are located in the spray area forward of the stagnation line such that they would deflect the oncoming spray down and aftward, thereby producing a reaction force that reduces the total resistance. An experimental study reported that the V-shaped spray interceptors to reduce the total resistance at low planing speed by up to 4%. This paper features a numerical comparison of two planing craft, one equipped with a conventional setup of longitudinal spray rails and the other with a V-shaped spray interceptor. Both configurations were simulated in calm water conditions and were free to pitch and heave in a speed range of Fr_∇ = 1.776 to 3.108. The numerical model was analyzed for grid sensitivity and numerical results were compared with experimental results. The two concepts were compared in terms of total resistance, lift, running position and wetted surface area. Conventional spray rails were shown to account for up to 5.6% of total lift and up to 6.5% of total resistance. The V-shaped spray interceptor was shown to reduce the total resistance by up to 8%. Since the V-shaped spray interceptor was located in the spray area forward of the stagnation line, it deflected the oncoming spray thereby producing a horizontal reaction force (-1.5% of R_{TM}) in the direction of the craft's motion. The rest of differences in the total resistance of the hulls equipped with the conventional spray rails and the V-shaped spray rails was due to absence of the resistance of the absent spray rails.

Keywords. Planing craft, spray rails, CFD, model tests data

1. Introduction

Whisker spray is the area of wetted bottom forward of the stagnation line of a planing craft. The direction of the fluid in the spray area is such that the streamlines are nearly a reflection of the free-stream about the stagnation line [1]. The resistance caused by spray has been shown to account for 10 - 25% of total resistance ($Fr_\nabla > 4$) by inference from a comparison of model test data of craft with and without spray rails [2–5]. Spray resistance is usually reduced by installing two to four longitudinal spray rails on the

[1] Corresponding Author, Miklos Lakatos, Estonian Maritime Academy, Tallinn University of Technology, Tallinna 19, 93819 Kuressaare, Estonia; E-mail: miklos.lakatos@taltech.ee

bottom of the hull. These rails detach the spray from the hull surface and deflect it towards the sides or slightly down and aftward, thereby reducing the frictional resistance by up to 18% [3].

A recent study suggests using spray deflectors that redirect the flow on the bottom of the craft and thereby recover spray energy to reduce the total resistance by up to 30% (compared to the bare hull) [6]. The spray deflectors are essentially a further iteration of the stepped hull concept that has been investigated significantly more than spray rails. Unlike the models used in [7] and [8], where the step was perpendicular to the keel, or [9], where the step had a forward sweep, in [6] the step was swept backwards. Besides, the step was located in the spray area forward of the stagnation such that it would deflect the oncoming spray down and aftward. Hence it is called deflector rather than a step. However, the study considered a hull with a constant deadrise at a fixed running position i.e. the influence of the spray deflectors on the craft's sinkage and pitch motion was neglected. The spray deflectors proposed in [6] were experimentally compared with conventional spray rails in model scale through towing tank testing in calm water and irregular waves [10]. The study reported that while the conventional spray rail setup reduced the total resistance by up to 9%, the spray deflectors reduced it by up to 20%.

A recent experimental study [11] compared a V-shaped spray interceptor (VSI) with conventional spray rails in calm water at $Fr_\nabla = 1.74 \ldots 3.26$. Although the VSI works essentially the same way as the spray deflectors do, there is a major difference between the two concepts. While the spray deflectors are in principle steps of a hull i.e. they are integral parts of the hull, the V-shaped spray interceptors are strips welded to the hull i.e. they are more like spray rails. The study reported that in planing regime the VSI reduced the total resistance of the craft by up to 4%, while conventional spray rails reduced it by up to 2%. The V-shaped spray interceptor was located in the spray area forward of the stagnation line such that it deflected the oncoming spray down, thereby producing a reaction force that reduced the total resistance, which confirmed the claims made in [6].

This study aims to further investigate the influence of the V-shaped spray interceptors [11] on the hydrodynamic characteristics of a planing craft in calm water and compare it with that of conventional spray rails. The numerical simulation allows analyzing phenomena (pressure distribution and wetted area) that are difficult to evaluate under experimental conditions. Finally, the numerical results of simulations of both hulls are compared with experimental data.

1.1. Test case

The object of this study is a test case vessel that has been designed the Small Craft Competence Centre (SCC) in Kuressaare, Estonia to compare conventional and novel spray rail configurations. The main particulars (Table 1) of the hull design are common for a high-speed patrol, search and rescue (SAR) vessel or a larger pleasure boat. The craft was designed to operate at a $Fr = 1.355$ and $Fr_\nabla = 3.108$, equivalent to the displacement of 40 t and speed of 35 knots in full scale.

The conventional spray rails arrangement (Figure 1a) was modelled with triangular 8x3mm profile (Figure 1b), with the deflection surface being horizontal. The V-shape arrangement (Figure 1c) was modelled with a triangular profile (Figure 1d) with the deflection surface perpendicular to the hull. The V-shaped spray interceptor was designed for $Fr = 1.355$ and $Fr_\nabla = 3.108$, equivalent to 40 t and 35 knots in full-scale.

Table 1. Main Dimensions of the test case hull.

Parameter		
Model Scale	λ	10
Length overall	L_{OA}	1.921 m
Length between perpendiculars	L_{PP}	1.800 m
Length waterline	L_{WL}	1.703 m
Beam overall	B_{OA}	0.581 m
Beam waterline	B_{WL}	0.581 m
Draught	T	0.108 m
Displacement mass	Δ_m	40 kg
Displacement volume	∇	0.040 m3
Longitudinal Centre of Gravity	L_{CG}	0.669 m
Vertical Centre of Gravity	KG	0.200 m

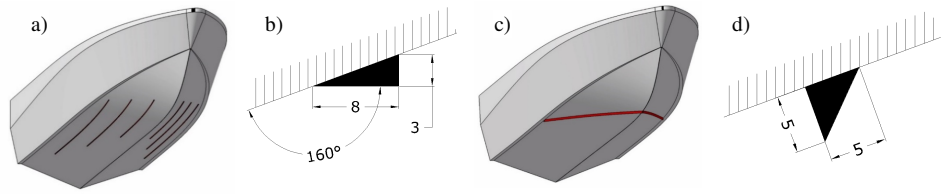

Figure 1. Spray rail configurations and their profiles: a) conventional spray rails (SR), b) 8x3 mm spray rail c) V-shaped spray interceptor (VSI), d) triangular 5x5mm interceptor.

2. Numerical model

The hydrodynamics of the planing hull was modelled using a commercial software Star-CCM+ v.15.02.007. An implicit unsteady solver was selected implementing RANS equations with k–ε turbulence model. The multiphase flow involving air and water is solved using the Volume of Fluid (VOF) approach that tracks the free surface boundary. The dynamic fluid-body interaction (DFBI) model was used for the evaluation of pitch and heave of the vessel. Main particulars of the numerical setup and the computational domain are shown in Table 2 and Figure 2 respectively.

The mesh is made of hexahedral control volumes and prism layer meshes are used for solving the flow in the boundary layer. The computational domain is divided into two regions: a stationary far-field region designated as "Tank" (Figure 3a) and a moving region designated as "Overset" (Figure 3b). The far-field region has three types of boundaries: Velocity Inlet, Pressure Outlet and Symmetry. The moving overset region has on the other hand: Wall, Symmetry and Overset. Since the model uses the overset grid and reference frame approach, the flow velocity is defined under reference frame and set to 0 in the Velocity Inlet boundary condition. The numerical model uses wave-damping for preventing wave reflection from the Inlet, outlet and side boundaries, with the wave damping length set to constant of 2.5 m from the boundary.

The time step Δt is controlled by a field function $\Delta t = CFL\,\Delta x/V_{Hull} = 0.25BS/V_{Hull}$, where Δx is the cell size (25% of the base size) the first level of refinement of the overset region and V_{Hull} the velocity of the hull. Hence, the field function defines the time step Δt such that the CFL=0.5 on the outer boundary and CFL=1 in the first level of refinement of the overset region. Hence, for the base size BS = 0.06m and Fr_∇ = 1.776 to 3.108 the respective time steps are $\Delta t = 0.008L_{pp}/V_{Hull}$,

which satisfies the ITTC recommendation [12] $\Delta t = 0.01 \sim 0.005\, l/V$, where l is characteristic length (in this case L_{PP}) and $V = V_{Hull}$ is the hull velocity.

A mesh sensitivity study was done to identify the minimum base size of the computational domain. Since the running trim of a planing craft is known to be extremely sensitive to generated lift, the grid sensitivity study was done on a craft with a fixed running position. Figure 4 shows that as the cell count increases, after base size $BS = 0.06m$ (1.9 million cells) the differences in total resistance were below 0.01%. Therefore, a base size $BS = 0.06m$ was selected for the rest of the simulations, resulting in 209,478 cells in the far-field region and 1,828,934 and 1,696,801 cells in the overset regions of the hulls equipped with spray rails and the V-shaped spray interceptors respectively. Figure 5 shows the distribution of wall y+ on the respective hulls.

Table 2. Solver settings

Item	Description
Convection Term	2nd order
Temporal Discretization	1st order
Time-step [s]	Function of velocity and mesh size
Inner iterations per time step	5
Turbulence model	Realizable k-ε
Overset interpolation scheme	Linear
Iterations of 6-DOF solver per inner iteration	3
Wall treatment	Two-Layer All y+

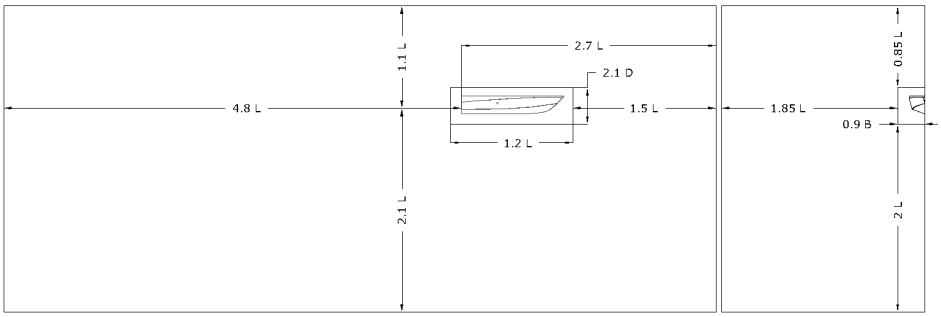

Figure 2. Dimensions of the simulation domain.

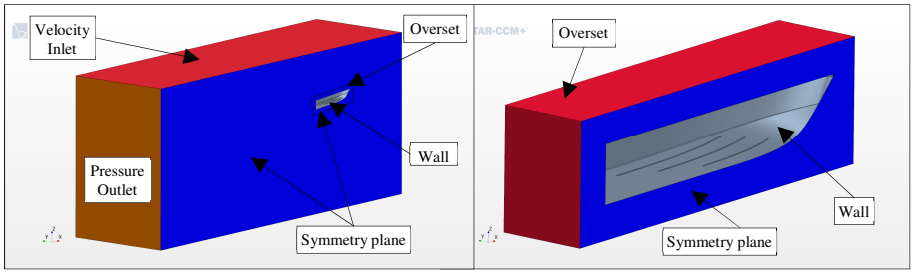

a) b)

Figure 3. Boundary conditions of the Tank (left) and Overset (right) regions.

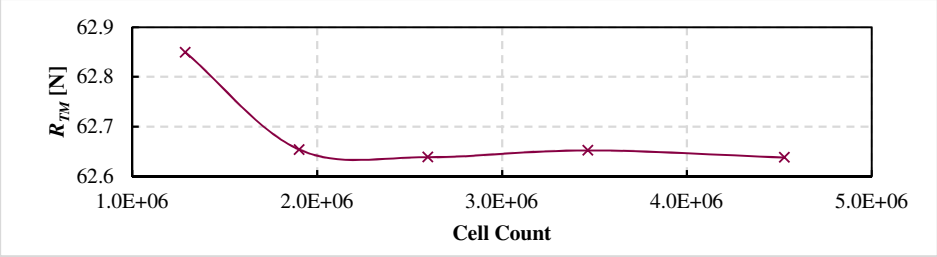

Figure 4. Grid sensitivity of total resistance.

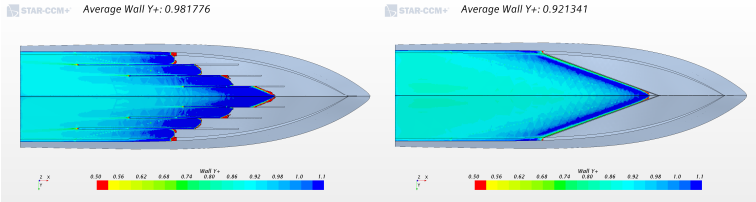

Figure 5. Wall Y+ on the hulls with spray rails (left) and the V-shaped spray interceptor (right) at Fr_∇=3.108.

3. Results and discussion

Figure 6 compares the vertical component of the lift L_V acting on the hull with conventional spray rails (SR) to that of the hull with the V-shaped spray interceptor (VSI). The differences in the lift were below 0.1% throughout the whole speed range, hence they were considered negligible.

When comparing the distribution of the vertical lift component on the individual hull parts at the top speed of $Fr_\nabla = 3.108$ (Figure 7), the spray rails were seen to account for a much larger lift than the V-shaped spray rail did. The spray rails produced 22N of vertical lift accounting for 6% of total lift, while the V-shaped spray interceptor only produced 1N of lift accounting for 0.3% of the latter. However, this difference in the lift on the spray rails and V-shaped spray interceptor was compensated by that of the bottom. The bottom of the hull equipped with V-shaped spray interceptor produced 19N more lift than the hull equipped with spray rails did. As for the chine, deck, keel, side and transom, no significant differences in the lift were observed.

Figure 8 compares the numerical and experimental values of the non-dimensional total resistance R_{TM}/Δ of the hull equipped with spray rails (SR) to those of the hull equipped and the V-shaped spray interceptor (VSI). Compared to model test results, the total resistance of the hull with spray rails (SR) was underestimated by 3% to 9%, while that of the hull with the VSI was underestimated by 6% to 8%. The most likely reason for the difference in resistance between the numerical and experimental results is the absence of the trimming moment due to towing force [13]. In the simulation the hull is moving relative to the background using reference frame method and the only forces acting on it are gravity and the hydrodynamic and hydrostatic forces that result in resistance and lift. In the experimental setup, on the other hand, besides the lift and drag, a towing force is acting at the towing point (x=0.36 m from the transom and z= 0.09 m from the baseline).

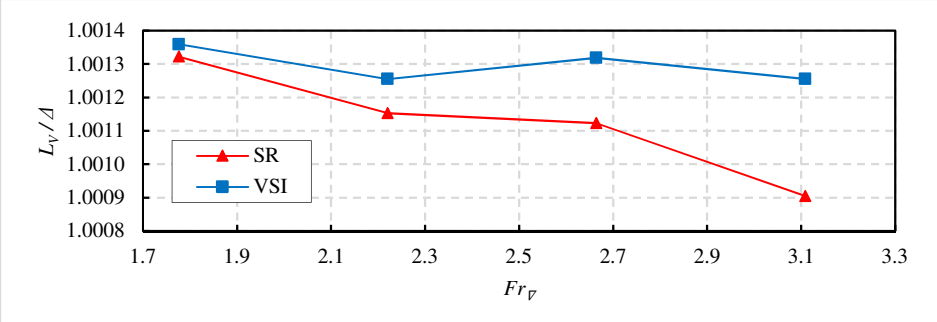

Figure 6. The vertical component of Lift.

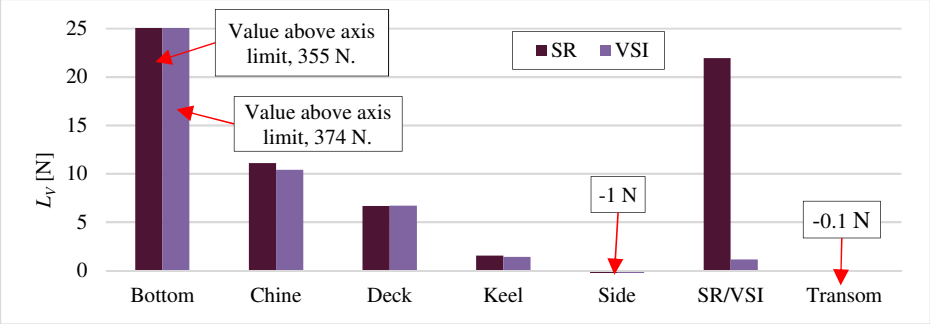

Figure 7. Distribution of the vertical component of the lift L_V on the hull at $Fr_\nabla = 3.108$.

Comparing numerical with experimental results, the general trends of resistance of the two hulls were rather similar. Compared to the hull with the spray rails, the total resistance of the hull with the V-shaped spray interceptor was significantly 7% and 8% lower at $Fr_\nabla = 2.66$ and $Fr_\nabla = 3.11$ and 1% and 6% higher at $Fr_\nabla = 1.77$ and $Fr_\nabla = 2.22$ respectively. However, it was observed that the differences in numerical total resistance were nearly twice as large as of those in experimental results.

Probably the most notable difference arose from the comparison of the total resistance of individual parts of the hull (Figure 9), in particular those of the spray rails and the V-shaped spray interceptor. The V-shaped spray interceptor accounted only for negative -1.3N (-1.5% of R_{TM}) resistance, while the spray rails accounted for 4.5N (6.5% of R_{TM}) of resistance. That is because the V-shaped spray interceptor was located in the spray area forward of the stagnation line such that it deflected the oncoming spray down, thereby producing a reaction force that reduced the total resistance.

It is important to note that since the VSI only produced a comparatively small reaction force (-1.5% of R_{TM}) in the direction of the hull's motion, the rest of the 8% difference was due to absence the of pressure and frictional resistance of the absent spray rails. As for the chine, deck, keel, side and transom, their resistance was negligibly smaller than that of the hull with spray rails. Figure 10 compares the pressure distribution of the hulls with the SR with those of the hull with the VSI. It was observed that at $Fr_\nabla = 1.77$ and $Fr_\nabla = 2.22$, the VSI gets in the way of the oncoming flow and causes a low-pressure area behind itself. This explains 1% and 6% higher total resistance compared to the hull with the spray rails.

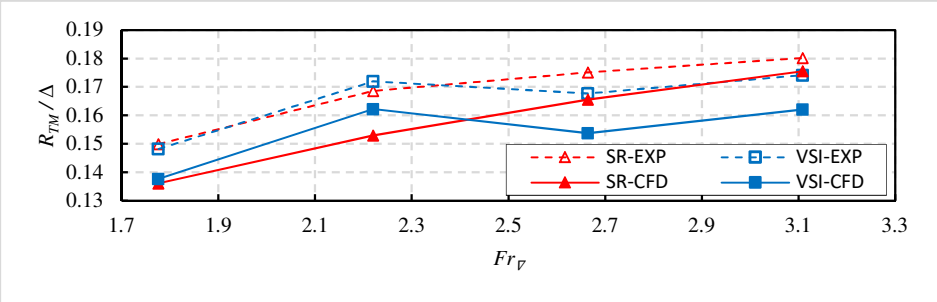

Figure 8. The total resistance of simulated configurations compared to model test results.

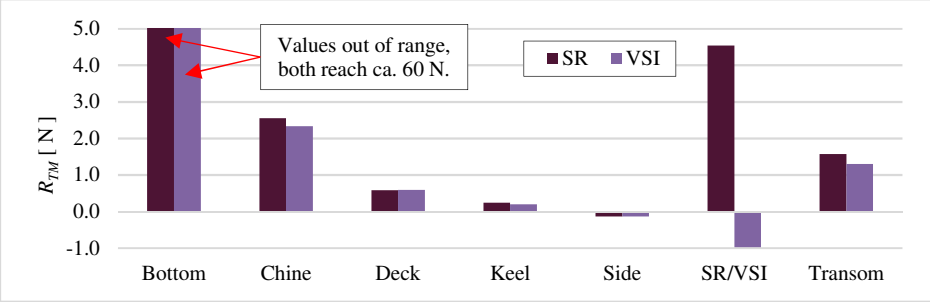

Figure 9. Distribution of the total resistance R_{TM} on the hull with conventional spray rails (SR) and V-shaped spray interceptor (VSI) at $Fr_\nabla = 3.108$.

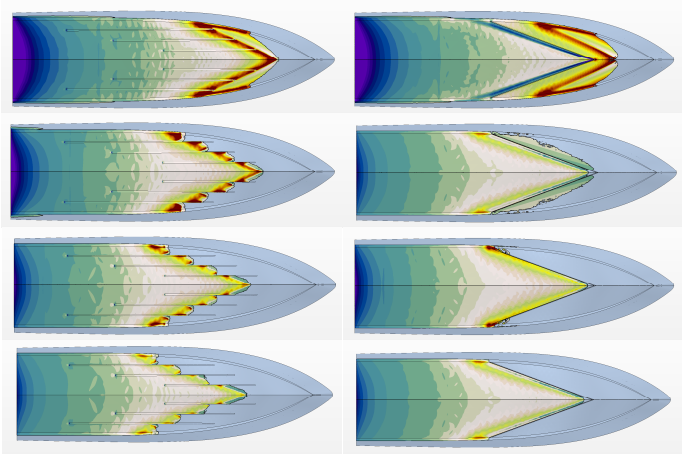

Figure 10. Pressure distribution of SR (left) and VSI (right) at Fr_∇ = 1.774 to 3.108 (top to bottom).

The running position of the simulated hulls is compared with that of model tests in terms of trim and sinkage in Figure 11 and Figure 12 respectively. While in the most cases trim was underestimated by around 0.6 to 0.9 degrees (13% to 16%), in the case of the hull equipped with the V-shaped spray interceptor (VSI) at $Fr_\nabla = 2.22$ the trim was underestimated by 1.4 degrees (25%). This outlier was also seen in the comparison of

sinkage. While in most cases sinkage was underestimated by 3mm to 6mm (9% to 12%), in the case of the hull with the VSI at $Fr_\nabla = 2.22$ sinkage was underestimated by 20mm (70%). Based on experimental data, the hull with the VSI was expected to have similar trim to that of the hull with spray rails (SR). Besides the absent moment due to towing force, a likely reason for that outlier is numerical ventilation observed in Figure 15.

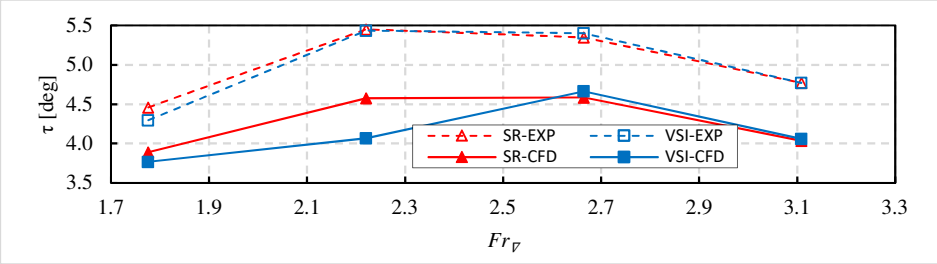

Figure 11. Trim of simulated configurations compared to model test results.

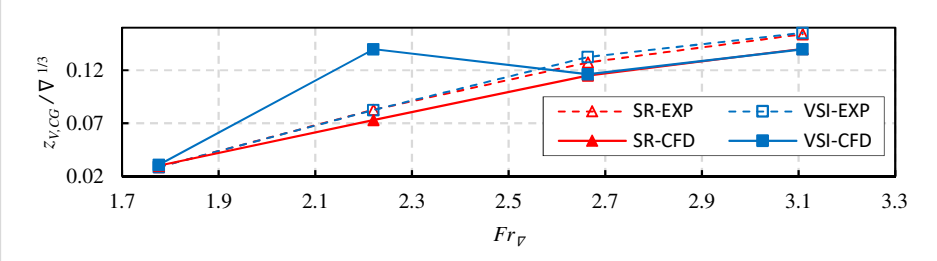

Figure 12. Non-dimensional sinkage of simulated configurations compared to model test results.

The wetted hull area underway S_{WHE} of the two simulated crafts was divided into the wetted bottom area S_{WB} and area wetted by the spray S_{WS}. S_{WB} was defined as the wetted area below the still water level ($z < 0$) while S_{WS} was defined as wetted are above still water level ($z > 0$) as shown in Figure 13 and Figure 14.

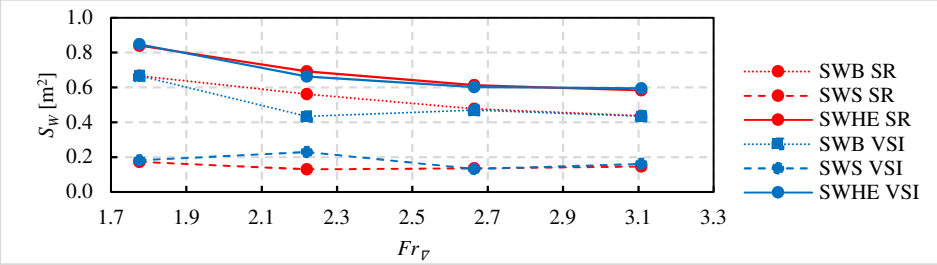

Figure 13. The wetted bottom area S_{WB}, area wetted by spray S_{WS} and wetted hull area underway S_{WHE}.

While the hull with the V-shaped spray interceptor was expected to significantly reduce the area wetted by spray, the numerical results show the opposite. No significant differences were observed in either S_{WB} or S_{WS}, except in the case of the hull with the VSI at $Fr_\nabla = 2.22$, where S_{WB} was lower and S_{WS} was higher those of the hull with the

SR. That is most likely due to the smaller than expected trim of hull with the VSI compared to the hull with the SR. Nevertheless, the differences in wetted hull area underway $S_{WHE} = S_{WB} + S_{WS}$ were between 1% and 4% through the whole speed range, hence marginal.

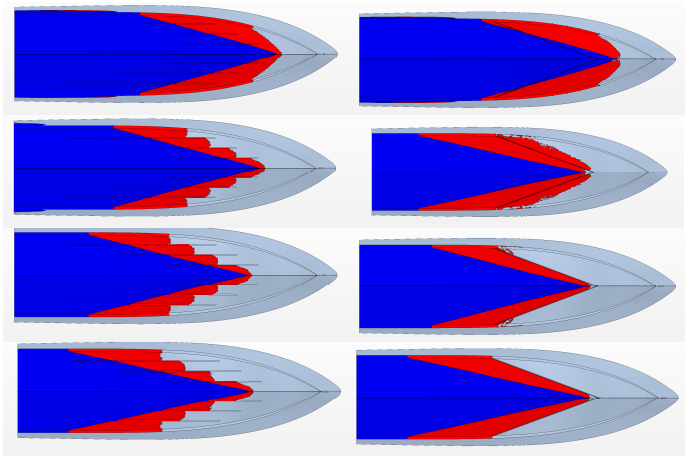

Figure 14. The wetted bottom area S_{WB} and area wetted by spray S_{WS} on SR (left) and VSI (right) at Fr_{∇} = 1.774 to 3.108 (top to bottom).

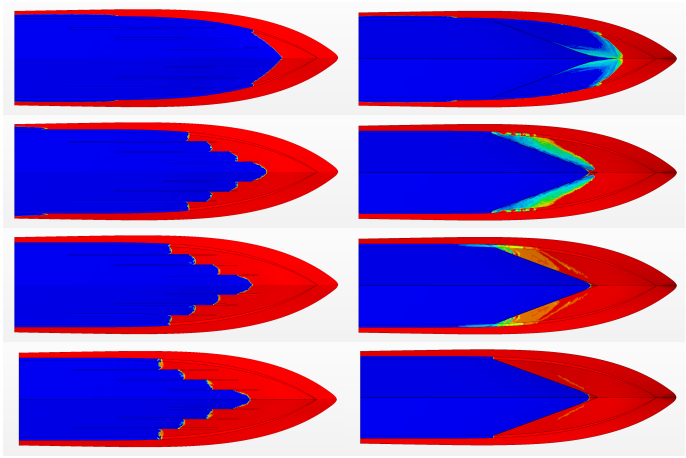

Figure 15. Volume Fraction of Air on SR (left) and VSI (right) at Fr_{∇} = 1.774 to 3.108 (top to bottom).

4. Conclusions

This paper presents a numerical analysis of two planing hulls in calm water, a hull equipped with conventional spray rails (SR) and one equipped with a novel V-shaped spray interceptor (VSI). The numerical results were compared with model test results and showed relatively good agreement. The main reason for the difference between numerical and experimental results was the absence of a moment due to the towing force in the numerical setup. Conventional spray rails were shown to account for up to 5.6%

of total lift and up to 6.5% of the total resistance in a speed range of $Fr_\nabla = 1.774 \ldots 3.108$. The V-shaped spray interceptor was shown to reduce the total resistance by up to 8%, compared to the hull with conventional spray rails. Since the VSI was located in the spray area slightly forward of the stagnation line such that it deflected the oncoming spray thereby producing a horizontal reaction force (-1.5% of R_{TM}) in the direction of the hull's motion. The rest of 8% differences in resistance of the hulls equipped with the SR and the VSI was due to absence the of resistance of the absent spray rails.

Future studies will investigate the influence of the width b_{SR} and the bottom angle δ of the spray rail as well as that of the V-shaped spray rail and chine interceptors on the hydrodynamics characteristics of the craft in calm water and waves. Furthermore, future studies will investigate the application of the Adaptive Mesh Refinement (AMR), a fairly new feature in the STAR-CCM+ software. AMR is particularly interesting since the perspective of achieving a high-resolution solution of the free surface and spray with a smaller number of cells is rather appealing.

References

[1] Savitsky D. Hydrodynamic design of planing hulls. Mar. Technol. 1964. p. 71–94.

[2] Clement EP. Effects of Longitudinal Bottom Spray Strips on Planing Boat Resistance, Report No.1818. Washington, DC.; 1964.

[3] Clement EP. Reduction of Planing Boat Resistance by Deflection of the Whisker Spray, Report No.1929. Washington, DC.; 1964.

[4] Grigoropoulos G, Loukakis T. Effect of Spray Rails on the Resistance of Planing Hulls. 3rd Intl Symp Fast Sea Transp FAST'95. Travenmuende, Germany; 1995.

[5] Grigoropoulos G. The use of Spray Rails and Wedges in Fast Monohulls. IV High-Speed Veh Intl Conf HSMV'97. Naples, Italy; 1997.

[6] Olin L, Altimira M, Danielsson J, et al. Numerical modelling of spray sheet deflection on planing hulls. Proc Inst Mech Eng Part M J Eng Marit Environ [Internet]. 2016. p. 811–817. Available from: http://journals.sagepub.com/doi/10.1177/1475090216682838.

[7] Taunton DJ, Hudson DA, Shenoi RA. Characteristics of A series of high speed hard chine planing hulls - Part 1: Performance in calm water. Int J Small Cr Technol [Internet]. 2010;152:55–75. Available from: http://eprints.soton.ac.uk/id/eprint/172717.

[8] Cucinotta F, Guglielmino E, Sfravara F. An experimental comparison between different artificial air cavity designs for a planing hull. Ocean Eng. 2017;140:233–243.

[9] De Marco A, Mancini S, Miranda S, et al. Experimental and numerical hydrodynamic analysis of a stepped planing hull. Appl Ocean Res [Internet]. 2017;64:135–154. Available from: http://dx.doi.org/10.1016/j.apor.2017.02.004.

[10] Molchanov B, Lundmark S, Fürth M, et al. Experimental validation of spray deflectors for high speed craft. Ocean Eng [Internet]. 2019;191:106482. Available from: https://doi.org/10.1016/j.oceaneng.2019.106482.

[11] Lakatos M, Sahk T, Kaarma R, et al. Experimental testing of spray rails for the resistance reduction of planing crafts. In: Soares CG, Parunov J, editors. Trends Anal Des Mar Struct Proc 7th Int Conf Mar Struct MARSTRUCT 2019. Dubrovnik: CRC Press/Balkema; 2019. p. 334–343.

[12] 28th ITTC. 7.5-03-02-03 Practical Guidelines for Ship CFD Applications. ITTC – Recomm Proced Guidel. 2017. p. 1–20.

[13] De Luca F, Mancini S, Pensa C, et al. Numerical evaluation (CFD) of Wake and Thrust deduction fraction of a Warped Hard Chine Hulls Systematic Series. 10th RINA High Speed Mar Veh Symp. 2014. p. 1–8.